HHS Public Access

Author manuscript

Prog Biophys Mol Biol. Author manuscript; available in PMC 2022 August 01.

Published in final edited form as:

Prog Biophys Mol Biol. 2021 August ; 163: 14–22. doi:10.1016/j.pbiomolbio.2020.10.007.

The dynamic nature of the Mre11-Rad50 DNA break repair complex

Mahtab Beikzadeh, **Michael P Latham**

Department of Chemistry and Biochemistry, Texas Tech University, Lubbock, TX, USA

Abstract

The Mre11-Rad50-Nbs1/Xrs2 protein complex plays a pivotal role in the detection and repair of DNA double strand breaks. Through traditional and emerging structural biology techniques, various functional structural states of this complex have been visualized; however, relatively little is known about the transitions between these states. Indeed, it is these structural transitions that are important for Mre11-Rad50-mediated DNA unwinding at a break and the activation of downstream repair signaling events. Here, we present a brief overview of the current understanding of the structure of the core Mre11-Rad50 complex. We then highlight our recent studies emphasizing the contributions of solution state NMR spectroscopy and other biophysical techniques in providing insight into the structures and dynamics associated with Mre11-Rad50 functions.

Keywords

Mre11-Rad50-Nbs1; DNA double strand break repair; DNA repair; Methyl TROSY; NMR spectroscopy; Allostery

1. Introduction

The primary focus of structural biology is often the three-dimensional structures of proteins and their complexes. Yet, to truly understand the function and mechanism of a protein at a molecular level, an accurate description for the movement of the atoms through space and time is required. All proteins experience small-scale fluctuations about their native states that are important for molecular recognition, catalytic, and allosteric events (Klinman, 2015; Stone, 2001). Other larger scale motions, such as the interconversions between conformational states, are also important for catalysis, ligand binding, and allostery (Boehr et al., 2009; Karplus and Kuriyan, 2005; Sekhar and Kay, 2019). In total, protein dynamics occurring on timescales ranging from picoseconds to seconds are critical for protein function. Thus, sophisticated experimental tools are needed to sample and interpret these

Corresponding author: Latham, Michael P (michael.latham@ttu.edu).

Mahtab Beikzadeh: Investigation, Writing - Original draft preparation, Writing - Review & Editing; **Michael Latham:** Conceptualization, Writing - Review & Editing, Supervision, Project administration, Funding acquisition.

motions. Within this toolbox, nuclear magnetic resonance (NMR) spectroscopy is unique in its ability to site-specifically reveal the presence of both small- and large-scale motions and to assign timescales to these dynamic processes (Boswell and Latham, 2019; Ortega et al., 2013; Palmer III, 2015).

The essential Mre11-Rad50-Nbs1/Xrs2 (MRN/X) complex is responsible in part for recognizing, signaling, and initiating the repair of DNA double strand breaks (DSBs) (Marsella et al., 2019; Paull, 2018; Syed and Tainer, 2018). Chromosomal DNA DSBs present a complex challenge for our cells, since the two ends of the broken DNA can diffuse away from one another and the template for proper repair is no longer in proximity. Failure to repair DNA DSBs can lead to mutation and genome instability, which are driving forces for many cancers (Rahman et al., 2020b). Cells rely on two major pathways to repair DNA DSBs: homologous recombination (HR) and nonhomologous end-joining (NHEJ) (Oh and Symington, 2018; Paull, 2018). The MRN/X complex plays a central and critical role in both of these repair pathways. MRN (or MRX in *S. cerevisiae*) is rapidly recruited to DNA DSBs, where it initiates DNA end resection and tethers the broken DNA ends for repair (Oh and Symington, 2018; Paull, 2018). MRN/X is also required to recruit and activate the protein kinase ATM (Tel1 in *S. cerevisiae*), which plays an essential role in DNA DSB signaling (Cassani et al., 2019; Deshpande et al., 2014; Lee et al., 2013). MRN is comprised of two Mre11, two Rad50, and one or two Nbs1 (also called Nibrin) subunits. The $Mre11_2$-$Rad50_2$ (MR) catalytic subcomplex (Fig. 1A) is conserved across all domains of life, while Nbs1/Xrs2 is only present in eukaryotes. Mre11 is a homodimer that has Mn^{2+}-dependent 3′-to-5′ exonuclease and ssDNA endonuclease activity (Hopfner et al., 2001; Matange et al., 2015). The endonuclease activity of Mre11 removes protein-DNA adducts (Hartsuiker et al., 2009; Neale et al., 2005). Specifically, Mre11 consists of a nuclease domain (light blue in Fig. 1A), which contains the active site; the capping domain (grey in Fig. 1A), which provides selectivity concerning DNA substrates; and a helix-loop-helix motif (purple in Fig. 1A), which binds to Rad50. Rad50, a member of the ATP-binding cassette (ABC)-ATPase superfamily of proteins, exhibits ATP binding and hydrolysis activities (Hopfner, 2016; Hopfner et al., 2000). It contains N- and C-terminal nucleotide binding sub-domains (red and gold in Fig. 1A), which fold together to form the functional nucleotide binding domain (NBD). Connecting these sub-domains is a long coiled-coil domain that forms extended arms culminating in an apical zinc hook domain. Rad50 binds the Mre11 helix-loop-helix motifs at the base of its coiled-coil domain and dimerizes via the zinc hook domain. Finally, the phosphopeptide-binding protein Nbs1/Xrs2 recruits downstream effector proteins to the site of the DNA DSB (Lloyd et al., 2009; Williams et al., 2009).

2. Structural transitions are important for MR function

Structural biology has revealed many of the conformations involved in MR function (Lafrance-Vanasse et al., 2015; Syed and Tainer, 2018). Notably, several high-resolution X-ray crystal structures have shown that the MR complex goes through large structural rearrangements minimally consisting of ATP-dependent association of the two Rad50 nucleotide binding domains (NBDs) and DNA-induced rotation of the Mre11 capping domains (Fig. 1). Rad50 ATP-dependent NBD association/dissociation (Lammens et al., 2011; Möckel et al., 2012), shown in Fig. 1A, is important for regulating MR activity. In the

ATP-free ‘open’ state, the Rad50 NBDs are disengaged, leaving the Mre11 nuclease active sites accessible to DNA substrate(s) (Lammens et al., 2011). Upon ATP binding, the two Rad50 protomers interact to form a compact ‘closed’ conformation (Lim et al., 2011; Möckel et al., 2012), sandwiching the two ATP molecules in the interface and forming a central groove on Rad50 that can accommodate double-stranded DNA (dsDNA) in a complex that is important not for DNA DSB repair but telomere length maintenance in yeast (Liu et al., 2016; Rojowska et al., 2014; Seifert et al., 2016). The ATP-bound closed form of MR occludes the DNA binding sites of Mre11 and is necessary for downstream signaling of the DNA DSB via ATM (Cassani et al., 2019; Deshpande et al., 2014; Lee et al., 2013). Rad50 ATP hydrolysis leads to the dissociation of the NBDs and is required for dsDNA unwinding and processive Mre11 exonuclease activity (Cannon et al., 2013; Herdendorf et al., 2011; Liu et al., 2016), suggesting that repetitive open-to-closed transitions are fundamental to the function of the complex.

Asymmetric Mre11 motions are another example of protein dynamics linked to MR function (Fig. 1B). There are numerous crystal structures of the Mre11 nuclease and capping domains ($Mre11^{ND}$) bound to DNAs that mimic DNA DSB or stalled replication fork substrates (Sung et al., 2014; Williams et al., 2008). Binding of a DNA DSB mimic to the *P. furiosus* (*Pf*) $Mre11^{ND}$ produced a symmetrical homodimer engaging two dsDNAs. However, a collapsed replication fork mimic yielded an asymmetric homodimer with only one bound DNA and different orientations for each $Mre11^{ND}$ capping domain. Based on these structures, a three step dynamic model (Fig. 1B) was proposed for DNA end processing (Williams et al., 2008). First, the Mre11 dimer interacts with the phosphates and minor groove of duplex DNA. Next, the capping domain rotates and a recognition loop wedges into the DNA minor groove, resulting in DNA melting. Finally, two conserved histidine residues facilitate phosphate bond rotation that directs the scissile strand over the Mre11 active site. The structures of the *M. jannaschii* (*Mj*) $Mre11^{ND}$ bound to longer DNAs also mimicking either a DNA DSB or stalled replication fork provided further insight into how DNA interacts with Mre11 (Sung et al., 2014). In these structures, both DNA substrates bound the Mre11 dimer asymmetrically via the extended duplex with only one substrate per dimer. The two capping domains move closer to each other upon DNA binding to enclose the DNA molecule between them, and the dimerization interface flexes to enable the engagement of Mre11 with the DNA. Here, it was proposed that the DNA end distant from the active site could be melted via interactions with a conserved basic patch on the surface of the nuclease domain and subsequent subunit rotation. This observation of asymmetric binding contrasts with the symmetric binding observed in *Pf* $Mre11^{ND}$; however, the two sets of structures could be visualizing different stages of the recognition of a DNA DSB by Mre11.

Recently, the cryo-electron microscopy “resolution revolution” has come for a bacterial MR complex in the form of structures of full-length *E. coli* MR (SbcCD) in the ATP-bound closed (“resting”) state and ADP-bound DNA “cutting” state (Käshammer et al., 2019), as shown in Fig. 1C. As observed in other ATP-bound closed MR structures (Lim et al., 2011; Möckel et al., 2012; Seifert et al., 2016), the Mre11 nuclease active sites were blocked (Fig. 1C, left); moreover, the Rad50 coiled-coils appeared flexible (i.e., were not visible during model construction). Of note, it was proposed that the ATP-bound closed state is the dominant form of the MR complex in the cell as the cellular concentration of ATP (~2 – 5

mM) and the Rad50 dissociation constant for ATP (K_D ~ 10 μM) suggest that Rad50 is always ATP-bound. Upon DNA binding, the two Rad50 coiled-coils zipped up into a rod and, together with the associated Rad50 NBDs, formed a clamp around the dsDNA. This architecture may explain how the coiled-coils act as clamps and a gate for detecting and processing diverse DNA ends (e.g., blunt, over-hang, or protein-DNA adducts). In the unique view of the "cutting" state, the Mre11 dimer moved to one side of Rad50 and assembled a DNA binding channel in conjunction with the central DNA binding groove formed by the associated NBDs (Fig. 1C, right). The DNA end was bound to one Mre11 exonuclease active site (Käshammer et al., 2019). These structures are distinct from the X-ray structures derived from the two different systems described above. In light of the cryo-EM structure, the X-ray data may reflect Mre11 structures that are important for DNA end bridging and/or DNA DSB scanning. Nevertheless, the cryo-EM structure elegantly explains the 3'−5' exonuclease activity of a bacterial MR complex and possibly uncovers a clamping and gating function for the coiled-coils.

3. Approaches for studying large protein complexes with solution state NMR

To bring the dynamics underlying the transitions between these various structures into focus, our laboratory studies the MR complex by solution state NMR spectroscopy coupled with biochemical and other biophysical assays. Technological and methodological advancements, such as ultra-high magnetic fields and the development of appropriate labeling schemes (e.g., deuteration), have made high quality NMR spectra of high molecular weight proteins and protein complexes (>40 kDa) possible. In fact, by leveraging the superior spectroscopic properties of $^{13}CH_3$-labeled side-chain methyl groups in an otherwise deuterated background, protein complexes > 1 MDa in size have been studied (Kay, 2011; Rosenzweig and Kay, 2014; Sprangers and Kay, 2007).

To investigate protein structure and dynamics using NMR, the observed peaks in the NMR spectra must first be assigned to specific side-chain methyl groups in the structure. Our NMR experiments utilize uniformly deuterated, side-chain methyl group Ileδ1-$^{13}CH_3$; Leuδ/Valγ−$^{13}CH_3$/$^{12}CD_3$; Metε−$^{13}CH_3$-labeled (referred to here as ILVM-labeled) protein samples coupled with methyl-Transverse Relaxation Optimized SpectroscopY (TROSY) (Tugarinov et al., 2003; Tugarinov and Kay, 2004) which together significantly improve both resolution and sensitivity of the spectra. Side-chain methyl group assignments are most often determined by comparison of experimental methyl-methyl distance observations from nuclear Overhauser effects (NOEs) data sets with theoretical distances calculated from crystal structures - in effect, doing the opposite of a traditional NMR structure calculation where peaks are assigned first using other methods and NOEs drive the structure determination. By changing the side-chain methyl group precursors in the growth media, additional samples can be produced to determine the intra-residue leucine/valine methyl groups (Sprangers and Kay, 2007), to determine stereochemistry (Gans et al., 2010), and to distinguish between leucine and valine residues (Lichtenecker et al., 2013). When ambiguities arise, point mutations are made to eliminate a specific peak from the spectrum allowing explicit assignment of that peak. Using this strategy, we have assigned ~98% and

~95% of the observed peaks in 2D correlation NMR spectra to ILVM methyl groups in the structures of *P. furious* (*Pf*) Mre11ND (a construct with only the nuclease and capping domains) and *Pf* Rad50^{NBD} (a construct where the coiled-coils and zinc hook have been omitted and the two ATPase subunits are connected via a flexible linker), respectively.

Since the NMR chemical shift (or resonance peak position) is extremely sensitive to the chemical environment of the probe nuclei, it is therefore sensitive to the conformational state of a biomolecule and can rapidly report on changes in structure upon ligand binding, modification, or mutation. Thus, a simple comparison of the methyl-TROSY spectra can be used to gain valuable structural information. It is to be expected that changes to the structure, and therefore the chemical shifts, will be observed near the site of perturbation. However, changes to the chemical shifts for residues distal to the site of perturbation are often indicative of correlated movements and possible allostery within the protein. Additionally, as is the case for traditional amide-based NMR methods, a variety of experiments exist for probing side-chain methyl group dynamics over the picosecond-to-days timescale (Boswell and Latham, 2019).

NMR is also an important tool in drug design and development. A number of successful drugs, available in the market or currently in clinical trials, originated from fragment-based drug design approaches where the ability of NMR to detect low affinity complexes is important (Hanzawa et al., 2020; Petros et al., 2006; Schoepfer et al., 2018). Moreover, NMR-derived structural models of protein-drug complexes have been used to further rational drug design, structure activity relationships, and hit to lead compound development (Hanzawa et al., 2020; Keiffer et al., 2020). For the MR complex, similar strategies could be employed to design small molecules that either disrupt nuclease or ATP hydrolysis function. For example, NMR studies on mirin-based inhibitors (Shibata et al., 2014) could further our understanding of their mechanisms of action against the nuclease activities of MRE11 and lead to the development of new compounds. On the other hand, specific inhibitors of RAD50 ATP hydrolysis function may be difficult to obtain because of the highly conserved nature of the ABC ATPase active site. Therefore, targeting unique conformational changes within the MR complex or the sub-states that lead to these changes could present an avenue for specific inhibitors. In fact, targeting protein-protein interactions and/or conformational changes has become a focus of many drug discovery programs (Dubey et al., 2020; Schoepfer et al., 2018). Since NMR spectroscopy can monitor these changes and sub-states (see below), it would be a powerful approach in the design of drugs targeting MR.

In our lab, we utilize the well-studied *Pf* MR as a model system because it is highly conserved in the MR functional motifs, the existing wealth of structural data allow us to put changes in NMR observables into a structural context, and its thermostability allows us to perform NMR experiments at high temperatures which improves the signal-to-noise ratio and resolution of our NMR data. Below are several examples of how we use NMR spectroscopy to study the structure and dynamics of the MR complex.

4. A dynamic allosteric network in Rad50 governs MR activity

In addition to the large global conformational changes that occur when Rad50 binds ATP (Fig. 1A), previous studies have indicated that the local rearrangement of salt-bridge and hydrogen bonding interactions within the Rad50 NBD upon ATP binding could also result in allostery with Mre11 and possibly the apical zinc hook, via the coiled-coil domain (Deshpande et al., 2014; Gao et al., 2016; Williams et al., 2011). The 'basic switch' residue (*Pf* Rad50 R805) in the extended signature helix forms critical interactions in the ATP-free state. Disruption of this basic switch via mutation altered Rad50 ATP hydrolysis activity and ATP-dependent association of the NBDs. This ultimately affected the ability of the MRN complex to repair DNA DSBs, providing potential evidence for long-range allostery (Deshpande et al., 2014; Williams et al., 2011). In the NMR spectra, we observe systematic chemical shift perturbations (CSPs; i.e., changes to the peak position) for many methyl groups in the R805E mutant. Mutations to the hinge region, which is structurally adjacent to the basic switch, showed similar CSPs (Fig. 2A) (Boswell et al., 2018). Notably, NMR spectroscopy was able to observe changes in the R805E structure where the static image from crystallography was unchanged from wild type (Deshpande et al., 2014), emphasizing that small structural changes and/or the interconversion of states can be detected with NMR. The peaks in the methyl-TROSY spectra moved linearly upon mutation, signifying that the observed peak position is a populated weighted average position between two rapidly interconverting conformations (i.e., fast exchange on the chemical shift timescale). We next applied chemical shift covariance analysis (CHESCA), a method for clustering residues undergoing fast exchange upon perturbation (here mutation) that has been used to identify allosteric networks within proteins (Boulton et al., 2014; Selvaratnam et al., 2011). CHESCA identified three clusters of methyl groups within Rad50 revealing an allosteric network that connects functional motifs across the protein.

As complementary functional data are essential when interpreting dynamic processes and their biological relevance, we also performed biochemical activity assays on $Rad50^{NBD}$ to determine the functional role of the allosteric network. Disrupting this network increased both the rate of ATP hydrolysis and ATP-induced Rad50 NBD association, which could be the result of either minimizing the energy barrier for $Rad50^{NBD}$ activity and/or increasing the population of an "active" $Rad50^{NBD}$ conformation (Fig. 2B). Furthermore, Mre11 exonuclease activity was also increased in the mutants.

We observed a clear correlation between changes in nanosecond timescale side-chain methyl group dynamics and increased ATP-induced NBD association, ATP hydrolysis, and Mre11 exonuclease activity; however, these fast timescale motions occur at least nine-orders of magnitude more rapidly than MR^{NBD} activity, which occurs on the minutes timescale. We are clearly not observing dynamics directly linked to these reactions. Thus, the question arises, what is the functional importance of these motions? In this case, the correlation may be indicative of a dynamic form of allostery rather than the more traditional structural form (Gunasekaran et al., 2004; Motlagh et al., 2014), whereby the increased flexibility limits the many stabilizing interactions that exist within Rad50 and governs its activity. Alternatively, the increased flexibility of side chains within this allosteric network could allow for the

functionally relevant state to become populated more rapidly, translating into increased activities.

Next, we questioned if the universally conserved D-loop motif also plays a role in this allosteric network (Boswell et al., 2020). Mutations of the conserved ABC ATPase D-loop leucine and aspartate residues in Rad50 have been observed in solid metastatic and breast cancer cells, respectively (Al-Ahmadie et al., 2014). In yeast, the leucine mutant results in loss of Tel1/ATM activation without affecting general DNA DSB repair, whereas the aspartate mutant led to cell death when exposed to DNA damage inducing drugs (Al-Ahmadie et al., 2014). Methyl-based NMR spectroscopy on the analogous mutants in *Pf* $Rad50^{NBD}$ (L828F and D829N) revealed that D829N only caused minor CSPs and changes to dynamics local to the D-loop and to nearby residues in the Rad50-Rad50 binding interface (Fig. 2A). Conversely, L828F produced CSPs and changes to dynamics to local methyl groups as well as to residues extending up to ~50 Å away, revealing that the allosteric network within Rad50 described above is also affected within this mutant. Thus, the adjacent L828F and D829N mutants had surprisingly different effects on the structure and dynamics of $Rad50^{NBD}$.

Unexpectedly, both *Pf* $Rad50^{NBD}$ D-loop mutants had faster ATP hydrolysis rates than wild type Rad50. The D-loop mutants gave somewhat lower Hill coefficients (though still >1) than wild type implying that they may disrupt the cooperativity between an ‘inactive’ and ‘active’ state within the ATP-bound closed conformation. It has previously been observed that dsDNA stimulates Rad50 ATP hydrolysis; we also observed faster hydrolysis rates for wild type and D-loop mutants in the presence of linearized dsDNA, although the degree of stimulation was far less for the mutants. We speculate that the increase in ATP hydrolysis rate in the presence of DNA could be the result of dsDNA binding acting as a positive allosteric regulator shifting the equilibrium of the ‘inactive’ and ‘active’ states. Together, these data provided strong evidence that the D-loop mutants partially eliminate cooperativity and allosteric regulation in Rad50 ATP hydrolysis.

5. Uncovering additional conformations of the MR complex in solution using LRET

To characterize the ATP-induced Rad50 NBD association/dissociation dynamics, we used Luminescence Resonance Energy Transfer (LRET) (Selvin, 2002; Zoghbi and Altenberg, 2018). LRET is a method similar to FRET whereby energy is transferred from a donor molecule (in this case a luminescent lanthanide) to an acceptor molecule in a distance dependent ($1/r^6$) manner. The lifetime of the donor-sensitized acceptor fluorescence intensity reports on the distance distributions between donor and acceptor probes within a complex as well as the population of molecules in each of the distributions (Fig. 2C). Wild type MR in the absence of ATP showed two conformations: a discrete ‘closed’ state consistent with the distances between the probes predicted from X-ray crystal structures with ATP/ATPγS (~38–40 Å) and a ‘partially open’ state (~48–54 Å; Figs. 2C and 2D). The fully ‘open’ state seen in X-ray crystal structures (Figs. 1A and 2D) and the newly proposed dissociated form of the Mre11 dimer (Käshammer et al., 2019; Saathoff et al., 2018; Sung et al., 2014; Tatebe

et al., 2020) were not detectable via LRET as the probes would be too far apart for efficient energy transfer. Addition of ATP shifted more molecules into the closed conformation; however, the partially open state was still observed even in the presence of saturating ATP (Fig. 2C).

LRET experiments on the D-loop mutants gave lower donor-sensitized acceptor emission as compared to the observed signal for wild type, suggesting a longer overall donor-acceptor distance and/or a smaller population of donor-acceptor pairs in proximity for the closed state. Upon analysis, the D-loop mutants also showed two discrete states, though with less of the population in the closed state and broader distributions in the partially open state. The addition of ATP did not shift as many molecules into the closed conformation as for wild type. Together, the biochemical, NMR, and LRET results reveal that the Rad50 D-loop mutants have gain-of-function ATP hydrolysis activity, while paradoxically having a smaller relative population of the ATP-induced closed conformation - the state from which ATP hydrolysis occurs.

In our studies of the basic switch/hinge and D-loop motifs, we observed how mutations that alter Rad50^{NBD} activity also change Mre11 activity. Although mutations to both regions accelerate ATP hydrolysis, they do so through different mechanisms: basic switch/hinge mutants appear to increase the rate of ATP-induced Rad50 NBD association (top arrow, Fig. 2B), whereas D-loop mutants appear to increase the population of ‘active’ Rad50 NBD (side arrow, Fig. 2B). Interestingly, Mre11 exonuclease activity increases with the basic switch/hinge mutants, which form more stably closed MR, and decreases with the D-loop mutants, which form less stably closed MR. Therefore, the flux through the ATP-induced Rad50^{NBD} closed state is important for Mre11 exonuclease activity. These observations are consistent with single molecule DNA unwinding experiments performed with human MRN complex, where it was demonstrated that ATP-induced association and/or hydrolysis was required for MRN-mediated dsDNA unwinding and subsequent resection (Cannon et al., 2013). They also determined that MRN containing a Rad50 signature motif mutant, which is incapable of ATP-induced closing and hydrolysis, does not support dsDNA unwinding or resection.

6. A stable Mre11 holds onto dsDNA for exonuclease reactions

We have also used NMR spectroscopy to understand how DNA DSB substrates affect the structure of Mre11 (Rahman et al., 2020a). To do this, we compared the methyl-TROSY spectra from unbound, ssDNA-, and dsDNA-bound *Pf* Mre11ND NMR samples. We observed only one set of peaks in the methyl-TROSY correlation spectra for ssDNA- or dsDNA-bound Mre11ND (Fig. 3A), implying that two DNAs interact symmetrically and stably with the Mre11ND dimer (one to each protomer). The spectral overlays showed different CSPs upon ssDNA and dsDNA binding, providing experimental evidence that ssDNA and dsDNA bind to Mre11ND differently (Fig. 3A). Generally, dsDNA caused CSPs mostly in the nuclease domain in agreement with the crystal structures of DNA-bound *Pf* and *Mj* Mre11ND, whereas ssDNA affected both the capping and nuclease domains consistent with the interactions noted in the *Pf* Mre11ND crystal structure with a branched DNA.

Several mutations and small molecule inhibitors have been described that result in an interesting exonuclease inactive/endonuclease active phenotype in Mre11 (Rahman et al., 2020a; Shibata et al., 2014; Williams et al., 2008). We have recently characterized the known *Pf* Mre11 H52S and a novel Y187C separation-of-nuclease function mutants (Rahman et al., 2020a). In fluorescence-based assays, we observed that these mutants do not change the affinity for dsDNA or ssDNA. However, comparison of methyl-TROSY correlation spectra showed that the chemical environment around the dsDNA recognition loops and the conserved basic patch in the nuclease domain were altered upon mutation (Fig. 3B). We therefore hypothesize that the separation-of-nuclease function might in part arise from improper recognition of the DNA end. Interestingly, we observed that these mutants changed the ps-to-ns timescale methyl group dynamics leading to a widespread increase in flexibility across $Mre11^{ND}$ (Fig. 3C). NMR-observed dsDNA melting experiments determined that the melting temperatures of the bound dsDNA in the mutant $Mre11^{ND}$-DNA complexes were lower than wild type complex indicating that the DNA helix is not as stable (Fig. 3D). Thus, these results suggest that Mre11 has evolved structurally and dynamically to properly recognize and then hold on to the DNA DSB substrate for subsequent exonuclease activity.

7. Other methods for studying the motions within the MR complex

Pioneering atomic force microscopy (AFM) studies by Wyman, Dekker, and colleagues over the last two decades have illuminated many architectural features of human MRN complexes (De Jager et al., 2001; Kinoshita et al., 2015; Moreno-Herrero et al., 2005; van Noort et al., 2003). Although not as high-resolution as other methods, AFM can visualize the overall structural shapes at the single molecule level and capture a range of steps in a dynamic process under relatively physiological conditions. In the case for the MRN complex, AFM has been one of the few structural techniques capable of probing the entire full-length complex. The authors initially demonstrated the general role of MR in tethering DNA molecules together, whereby the MR complex provides a bridge between DNA ends (De Jager et al., 2001). In a subsequent study, they developed a method to quantify local flexibility from high-resolution AFM images. From the calculated flexibility maps of RAD50, two positions of high flexibility within the RAD50 coiled-coils were identified (van Noort et al., 2003). It was proposed that these flexible regions would enable the apical zinc hook ends of multiple DNA-bound MR complexes to form intermolecular interactions independent of the orientation of their DNA-bound globular domains. It was also noticed that DNA binding by the MRN globular domain led to parallel orientation of the coiled-coils which favors the inter-complex associations needed for DNA tethering (Moreno-Herrero et al., 2005). Notably, a parallel orientation of the coiled-coils was also observed in the recent cryo-EM structure of DNA-bound *E. coli* MR complex described above (Käshammer et al., 2019).

Henderson and co-workers have recently investigated the MR complex from the thermophilic archaeon *Sulfolobus acidocaldarius* using real-time AFM (Zabolotnaya et al., 2020). Whereas earlier studies only described interactions between the globular domains of MR and DNA (see above), they visualized an additional and novel interaction between the DNA and the Rad50 coiled-coils. Measuring the distance between wild type MR and

MR(Δcc) (a Rad50 construct with truncated coiled coils but still containing the native zinc hook region) complexes and a dsDNA end, they observed that wild type complexes have a statistically significant preference for binding to free dsDNA ends which was not the case for the MR(Δcc) mutant. Moreover, the MR(Δcc) complexes failed to form DNA loops or bridges between two or more DNA ends. Together, these results suggested that the full-length coiled-coil domains are important for the localization of MR complexes at the dsDNA ends and for tethering two DNA ends together. Next, the DNA binding activity of the MR complexes was monitored over a 30 min period. The Rad50 coiled-coil region adjacent to the apical zinc hook and the DNA substrate engaged in dynamic interactions during which the complex seemed to scan the DNA until it found the end. These results might complement single-molecule FRET studies which demonstrated that full length MR complexes can diffuse along DNA packaged in nucleosomes whereas a construct similar to MR(Δcc) could not (Myler et al., 2017).

In contrast to the studies discussed above, Furukohri and co-workers have recently observed via AFM that the RAD50 coiled-coils appear to be in constant contact at the zinc hook domain, whereas the catalytic, globular head domain occasionally dissociates, presumably at the MRE11 dimerization interface (Tatebe et al., 2020). This head open structure has previously been proposed from biochemical assays (Käshammer et al., 2019; Saathoff et al., 2018; Sung et al., 2014). Because the RAD50 zinc hook resembles the hinge domains from other SMC family members, the zinc hook was replaced with the SMC hinge from the bacterial condensin MukB, which maintains a stable dimer. This chimera Rad50 was fully functional in repairing DNA damage in yeast, suggesting that, like the SMC hinge, the Rad50 zinc hook is a stable dimerization interface and that zinc hook dissociation is not required for DNA DSB repair.

From these and other studies, it is becoming increasingly clear that protein motions are a key feature of MR function; therefore, other techniques are also being applied to the complex to understand the connection between dynamics and function. Like NMR spectroscopy, molecular dynamics (MD) simulations in the past have suffered from a size problem; however, advances in hardware and software have made MD simulations on the 100's ns to 5 μs timescale possible for systems as large as the MR complex. Two recent studies have made use of MD simulations on the yeast MR^{NBD} complex to understand the ATP-dependent activation of ATM/Tel1. Longhese and co-workers performed MD simulations starting from ATP- or ADP-bound closed structures of wild type yeast MR^{NBD} and compared these to a Rad50 mutant (A78T) that affects Tel1 activation (Cassani et al., 2019). First, MD simulations on ATP-bound MR^{NBD} confirmed that the two $Rad50^{NBD}$ protomers are tightly bound with the two ATP molecules buried in the interface. In contrast, the conformations observed for ADP-bound MR^{NBD} are not as tightly bound as the two $Rad50^{NBD}$ protomers have moved apart. Thus, as expected, ATP hydrolysis appears to decrease the affinity of the $Rad50^{NBD}$ protomers for each other. Interestingly, these MD simulations suggested an asymmetric opening of closed $Rad50^{NBD}$, with the first active site opening inducing the opening of the second. Asymmetric opening of $Rad50^{NBD}$ is one potential mechanism for the cooperativity and allosteric activation observed in $Rad50^{NBD}$ ATP hydrolysis. It was also observed that ADP weakened the interactions between $Rad50^{NBD}$ and Mre11, which would also help promote an opening of the closed form. MD simulations performed on MR^{NBD}

containing the Rad50 A78T substitution generally showed less of the stably closed state. In fact, the ATP-bound mutant MR^{NBD} sampled states where $Rad50^{NBD}$ was disengaged from the Mre11 nuclease sites. The lack of a stably closed ATP-bound state could explain the action of this separation-of-function Rad50 mutant (i.e., no effect on DNA DSB repair but impaired Tel1 activation). Petrini and co-workers have also performed MD simulations on the closed (ATPγS-bound) yeast MR^{NBD} to explore the structural and dynamics basis for another $Rad50^{NBD}$ separation-of-function mutant, D67N/Y (Hohl et al., 2020). In this case, the mutant had increased contact times with the nucleotide. From these data, the authors hypothesize that ADP release may be impaired in the mutant altering the dynamics of MR^{NBD} transitioning from the closed to the open form. They further speculate that it is the transition between the closed and open forms of MR^{NBD} that is important for the activation of ATM/Tel1 rather than the actual states themselves.

As mentioned above, single molecule fluorescence methods have been used to examine MRN dsDNA unwinding and sliding of the complex along DNA (Cannon et al., 2013; Deshpande et al., 2020; Myler et al., 2017). From the latter, lifetimes have been determined for the occupation of the MRN complex and a variety of other DNA DSB repair proteins (e.g., Ku and DNA-PKcs) on the DNA (Deshpande et al., 2020; Myler et al., 2017). A particularly powerful use of this approach has been to compare these lifetimes in the absence or presence of other factors, for example nucleosomes, which has allowed direct observation for the order of operations at a DNA DSB. Notably, single molecule FRET studies are well suited for studying the structure and dynamics of the metazoan MRN complex, for which obtaining large quantities of proteins for structural studies is difficult.

8. Conclusion and Future Directions

Elegant structures of the MR complex have laid a foundation for our understanding of the different conformational states related to its role DNA DSB repair. The MRN community seeks to build on these with a dynamic picture of the transitions within and between these structures, as these motions are intricately involved in the enzymatic activity of the protein complex. These motions may also be important for signaling the presence of DNA DSBs (Cassani et al., 2019; Deshpande et al., 2014; Lee et al., 2013), and their disruption have been associated with disease (Boswell et al., 2020; Hohl et al., 2020); therefore, the characterization of the transitions between states is as important to understanding the effects of mutations as static structures. In the examples from our laboratory presented here, changes in chemical shift positions and dynamics from NMR experiments informed us about an allosteric network within Rad50 and gave insight for how Mre11 interacts with DNA. Other studies utilizing AFM, molecular dynamics studies, and single molecule FRET also illuminate local and global structural changes within the MRN complex that are necessary for function. Yet, there are still many unanswered questions about the interplay of MR structure, dynamics, and function. For example, structures are absent for the complex bound to other relevant DNA substrates (e.g., ssDNA or protein-DNA adducts). Also, a complete understanding of the role of ATP hydrolysis, the function of opening and closing, allostery through the Rad50 coiled-coil domains, and the new ‘partially open’ state of the complex is still lacking.

Acknowledgements

We also thank Marella Canny for help editing and the other members of the Latham laboratory for their input regarding this manuscript.

Funding

We thank the Welch Foundation (D-1876; 2015 - present), Cancer Prevention and Research Institute of Texas (RP180553; 2018 - present), and the National Institute of General Medical Sciences (1R35GM128906; 2018 - present) for support of our research into the structures, dynamics, and function of the Mre11-Rad50 complex.

References

Al-Ahmadie H, Iyer G, Hohl M, Asthana S, Inagaki A, Schultz N, Hanrahan AJ, Scott SN, Brannon AR, McDermott GC, Pirun M, Ostrovnaya I, Kim P, Socci ND, Viale A, Schwartz GK, Reuter V, Bochner BH, Rosenberg JE, Bajorin DF, Berger MF, Petrini JHJ, Solit DB, Taylor BS, 2014. Synthetic Lethality in ATM-Deficient RAD50-Mutant Tumors Underlies Outlier Response to Cancer Therapy. Cancer Discov. 4, 1014–1021. 10.1158/2159-8290.CD-14-0380 [PubMed: 24934408]

Boehr DD, Nussinov R, Wright PE, 2009. The role of dynamic conformational ensembles in biomolecular recognition. Nat. Chem. Biol 5, 789–796. 10.1038/nchembio.232 [PubMed: 19841628]

Boswell ZK, Canny MD, Buschmann TA, Sang J, Latham MP, 2020. Adjacent mutations in the archaeal Rad50 ABC ATPase D-loop disrupt allosteric regulation of ATP hydrolysis through different mechanisms. Nucleic Acids Res 48, 2457–2472. 10.1093/nar/gkz1228 [PubMed: 31889185]

Boswell ZK, Latham MP, 2019. Methyl-Based NMR Spectroscopy Methods for Uncovering Structural Dynamics in Large Proteins and Protein Complexes. Biochemistry 58, 144–155. 10.1021/acs.biochem.8b00953 [PubMed: 30336000]

Boswell ZK, Rahman S, Canny MD, Latham MP, 2018. A dynamic allosteric pathway underlies Rad50 ABC ATPase function in DNA repair. Sci. Rep 8, 1–12. 10.1038/s41598-018-19908-8 [PubMed: 29311619]

Boulton S, Akimoto M, Selvaratnam R, Bashiri A, Melacini G, 2014. A tool set to map allosteric networks through the NMR chemical shift covariance analysis. Sci. Rep 4, 7306. 10.1038/srep07306 [PubMed: 25482377]

Cannon B, Kuhnlein J, Yang S-H, Cheng A, Schindler D, Stark JM, Russell R, Paull TT, 2013. Visualization of local DNA unwinding by Mre11/Rad50/Nbs1 using single-molecule FRET. Proc. Natl. Acad. Sci. U. S. A 110, 18868–73. 10.1073/pnas.1309816110 [PubMed: 24191051]

Cassani C, Vertemara J, Bassani M, Marsella A, Tisi R, Zampella G, Longhese MP, 2019. The ATP-bound conformation of the Mre11-Rad50 complex is essential for Tel1/ATM activation. Nucleic Acids Res. 47, 3550–3567. 10.1093/nar/gkz038 [PubMed: 30698745]

De Jager M, Van Noort J, Van Gent DC, Dekker C, Kanaar R, Wyman C, 2001. Human Rad50/Mre11 is a flexible complex that can tether DNA ends. Mol. Cell 8, 1129–1135. 10.1016/S1097-2765(01)00381-1 [PubMed: 11741547]

Deshpande RA, Myler LR, Soniat MM, Makharashvili N, Lee L, Lees-Miller SP, Finkelstein IJ, Paull TT, 2020. DNA-dependent protein kinase promotes DNA end processing by MRN and CtIP. Sci. Adv 6. 10.1126/sciadv.aay0922

Deshpande RA, Williams GJ, Limbo O, Williams RS, Kuhnlein J, Lee J-H, Classen S, Guenther G, Russell P, Tainer JA, Paull TT, 2014. ATP-driven Rad50 conformations regulate DNA tethering, end resection, and ATM checkpoint signaling. EMBO J. 33, 482–500. 10.1002/embj.201386100 [PubMed: 24493214]

Dubey A, Takeuchi K, Reibarkh M, Arthanari H, 2020. The role of NMR in leveraging dynamics and entropy in drug design. J. Biomol. NMR 10.1007/s10858-020-00335-9

Gans P, Hamelin O, Sounier R, Ayala I, Durá MA, Amero CD, Noirclerc-Savoye M, Franzetti B, Plevin MJ, Boisbouvier J, 2010. Stereospecific Isotopic Labeling of Methyl Groups for NMR

Spectroscopic Studies of High-Molecular-Weight Proteins. Angew. Chemie Int. Ed 49, 1958–1962. 10.1002/anie.200905660

Gao Y, Meyer JR, Nelson SW, 2016. A network of allosterically coupled residues in the bacteriophage T4 Mre11-Rad50 complex. Protein Sci. 25, 2054–2065. 10.1002/pro.3028 [PubMed: 27571435]

Gunasekaran K, Ma B, Nussinov R, 2004. Is allostery an intrinsic property of all dynamic proteins? Proteins 57, 433–43. 10.1002/prot.20232 [PubMed: 15382234]

Hanzawa H, Shimada T, Takahashi M, Takahashi H, 2020. Revisiting biomolecular NMR spectroscopy for promoting small-molecule drug discovery. J. Biomol. NMR 10.1007/s10858-020-00314-0

Hartsuiker E, Neale MJ, Carr AM, 2009. Distinct Requirements for the Rad32Mre11 Nuclease and Ctp1CtIP in the Removal of Covalently Bound Topoisomerase I and II from DNA. Mol. Cell 33, 117–123. 10.1016/j.molcel.2008.11.021 [PubMed: 19150433]

Herdendorf TJ, Albrecht DW, Benkovic SJ, Nelson SW, 2011. Biochemical characterization of bacteriophage T4 Mre11-Rad50 complex. J. Biol. Chem 286, 2382–2392. 10.1074/jbc.M110.178871 [PubMed: 21081488]

Hohl M, Mojumdar A, Hailemariam S, Kuryavyi V, Ghisays F, Sorenson K, Chang M, Taylor BS, Patel DJ, Burgers PM, Cobb JA, Petrini JHJ, 2020. Modeling cancer genomic data in yeast reveals selection against ATM function during tumorigenesis. PLoS Genet. 16, 1–28. 10.1371/journal.pgen.1008422

Hopfner K-P, 2016. Invited review: Architectures and mechanisms of ATP binding cassette proteins. Biopolymers 105, 492–504. 10.1002/bip.22843 [PubMed: 27037766]

Hopfner K-P, Karcher A, Craig L, Woo TT, Carney JP, Tainer JA, 2001. Structural biochemistry and interaction architecture of the DNA double-strand break repair Mre11 nuclease and Rad50-ATPase. Cell 105, 473–85. [PubMed: 11371344]

Hopfner K-P, Karcher A, Shin DS, Craig L, Arthur LM, Carney JP, Tainer JA, 2000. Structural biology of Rad50 ATPase: ATP-driven conformational control in DNA double-strand break repair and the ABC-ATPase superfamily. Cell 101, 789–800. [PubMed: 10892749]

Karplus M, Kuriyan J, 2005. Molecular dynamics and protein function. Proc. Natl. Acad. Sci. U. S. A 102, 6679–6685. 10.1073/pnas.0408930102 [PubMed: 15870208]

Käshammer L, Saathoff J-H, Lammens K, Gut F, Bartho J, Alt A, Kessler B, Hopfner K-P, 2019. Mechanism of DNA End Sensing and Processing by the Mre11-Rad50 Complex. Mol. Cell 76, 382–394.e6. 10.1016/j.molcel.2019.07.035 [PubMed: 31492634]

Kay LE, 2011. Solution NMR spectroscopy of supra-molecular systems, why bother? A methyl-TROSY view. J. Magn. Reson 210, 159–170. 10.1016/j.jmr.2011.03.008 [PubMed: 21458338]

Keiffer S, Carneiro MG, Hollander J, Kobayashi M, Pogoryelev D, AB E, Theisgen S, Müller G, Siegal G, 2020. NMR in target driven drug discovery: why not? J. Biomol. NMR 1, 3. 10.1007/s10858-020-00343-9

Kinoshita E, Van Rossum-Fikkert S, Sanchez H, Kertokalio A, Wyman C, 2015. Human RAD50 makes a functional DNA-binding complex. Biochimie 113, 47–53. 10.1016/j.biochi.2015.03.017 [PubMed: 25828805]

Klinman JP, 2015. Dynamically achieved active site precision in enzyme catalysis. Acc. Chem. Res 48, 449–56. 10.1021/ar5003347 [PubMed: 25539048]

Lafrance-Vanasse J, Williams GJ, Tainer JA, 2015. Envisioning the dynamics and flexibility of Mre11-Rad50-Nbs1 complex to decipher its roles in DNA replication and repair. Prog. Biophys. Mol. Biol 117, 182–193. 10.1016/j.pbiomolbio.2014.12.004 [PubMed: 25576492]

Lammens K, Bemeleit DJ, Möckel C, Clausing E, Schele A, Hartung S, Schiller CB, Lucas M, Angermüller C, Söding J, Sträßer K, Hopfner K-P, 2011. The Mre11:Rad50 structure shows an ATP-dependent molecular clamp in DNA double-strand break repair. Cell 145, 54–66. 10.1016/j.cell.2011.02.038 [PubMed: 21458667]

Lee J-H, Mand MR, Deshpande RA, Kinoshita E, Yang S-H, Wyman C, Paull TT, 2013. Ataxia Telangiectasia-Mutated (ATM) Kinase Activity Is Regulated by ATP-driven Conformational Changes in the Mre11/Rad50/Nbs1 (MRN) Complex. J. Biol. Chem 288, 12840–12851. 10.1074/jbc.M113.460378 [PubMed: 23525106]

Lichtenecker RJ, Weinhäupl K, Reuther L, Schörghuber J, Schmid W, Konrat R, 2013. Independent valine and leucine isotope labeling in Escherichia coli protein overexpression systems. J. Biomol. NMR 57, 205–209. 10.1007/s10858-013-9786-y [PubMed: 24078042]

Lim HS, Kim JS, Park YB, Gwon GH, Cho Y, 2011. Crystal structure of the Mre11-Rad50-ATPγS complex: understanding the interplay between Mre11 and Rad50. Genes Dev. 25, 1091–104. 10.1101/gad.2037811 [PubMed: 21511873]

Liu Y, Sung S, Kim Y, Li F, Gwon G, Jo A, Kim T, Song O-K, Lee SE, Cho Y, Kim A, 2016. ATP-dependent DNA binding, unwinding, and resection by the Mre11/Rad50 complex. EMBO J. 35, 1–16. 10.15252/embj.201592462 [PubMed: 26567170]

Lloyd J, Chapman JR, Clapperton JA, Haire LF, Hartsuiker E, Li J, Carr AM, Jackson SP, Smerdon SJ, 2009. A supramodular FHA/BRCT-repeat architecture mediates Nbs1 adaptor function in response to DNA damage. Cell 139, 100–11. 10.1016/j.cell.2009.07.043 [PubMed: 19804756]

Marsella A, Cassani C, Casari E, Tisi R, Longhese MP, 2019. Structure-function relationships of the Mre11 protein in the control of DNA end bridging and processing. Curr. Genet 65, 11–16. 10.1007/s00294-018-0861-5 [PubMed: 29922906]

Matange N, Podobnik M, Visweswariah SS, 2015. Metallophosphoesterases: structural fidelity with functional promiscuity. Biochem. J 467, 201–216. 10.1042/BJ20150028 [PubMed: 25837850]

Möckel C, Lammens K, Schele A, Hopfner K-P, Pemberton T, 2012. ATP driven structural changes of the bacterial Mre11:Rad50 catalytic head complex. Nucleic Acids Res. 40, 914–27. 10.1093/nar/gkr749 [PubMed: 21937514]

Moreno-Herrero F, De Jager M, Dekker NH, Kanaar R, Wyman C, Dekker C, 2005. Mesoscale conformational changes in the DNA-repair complex Rad50/Mre11/Nbs1 upon binding DNA. Nature 437, 440–3. 10.1038/nature03927 [PubMed: 16163361]

Motlagh HN, Wrabl JO, Li J, Hilser VJ, 2014. The ensemble nature of allostery. Nature 508, 331–339. 10.1038/nature13001 [PubMed: 24740064]

Myler LR, Gallardo IF, Soniat MM, Deshpande RA, Gonzalez XB, Kim Y, Paull TT, Finkelstein IJ, 2017. Single-Molecule Imaging Reveals How Mre11-Rad50-Nbs1 Initiates DNA Break Repair. Mol. Cell 67, 891–898.e4. 10.1016/j.molcel.2017.08.002 [PubMed: 28867292]

Neale MJ, Pan J, Keeney S, 2005. Endonucleolytic processing of covalent protein-linked DNA double-strand breaks. Nature 436, 1053–1057. 10.1038/nature03872 [PubMed: 16107854]

Oh J, Symington LS, 2018. Role of the Mre11 complex in preserving genome integrity. Genes (Basel). 9, 1–25. 10.3390/genes9120589

Ortega G, Pons M, Millet O, 2013. Protein Functional Dynamics in Multiple Timescales as Studied by NMR Spectroscopy, 1st ed, Dynamics of Proteins and Nucleic Acids. Copyright © 2013 Elsevier Inc. All rights reserved. 10.1016/B978-0-12-411636-8.00006-7

Palmer III AG, 2015. Enzyme Dynamics from NMR Spectroscopy. Acc. Chem. Res 48, 457–465. 10.1021/ar500340a [PubMed: 25574774]

Paull TT, 2018. 20 Years of Mre11 Biology: No End in Sight. Mol. Cell 71, 419–427. 10.1016/j.molcel.2018.06.033 [PubMed: 30057197]

Petros AM, Dinges J, Augeri DJ, Baumeister SA, Betebenner DA, Bures MG, Elmore SW, Hajduk PJ, Joseph MK, Landis SK, Nettesheim DG, Rosenberg SH, Shen W, Thomas S, Wang X, Zanze I, Zhang H, Fesik SW, 2006. Discovery of a potent inhibitor of the antiapoptotic protein Bcl-X L from NMR and parallel synthesis. J. Med. Chem 49, 656–663. 10.1021/jm0507532 [PubMed: 16420051]

Rahman S, Beikzadeh M, Canny MD, Kaur N, Latham MP, 2020a. Mutation of Conserved Mre11 Residues Alter Protein Dynamics to Separate Nuclease Functions. J. Mol. Biol 432, 3289–3308. 10.1016/j.jmb.2020.03.030 [PubMed: 32246962]

Rahman S, Canny MD, Buschmann TA, Latham MP, 2020b. A Survey of Reported Disease-Related Mutations in the MRE11-RAD50-NBS1 Complex. Cells 9, 1678. 10.3390/cells9071678

Rojowska A, Lammens K, Seifert FU, Direnberger C, Feldmann H, Hopfner K-P, 2014. Structure of the Rad50 DNA double-strand break repair protein in complex with DNA. EMBO J. 33, 2847–59. 10.15252/embj.201488889 [PubMed: 25349191]

Rosenzweig R, Kay LE, 2014. Bringing dynamic molecular machines into focus by methyl-TROSY NMR. Annu. Rev. Biochem 83, 291–315. 10.1146/annurev-biochem-060713-035829 [PubMed: 24905784]

Saathoff J-H, Käshammer L, Lammens K, Byrne RT, Hopfner K-P, 2018. The bacterial Mre11–Rad50 homolog SbcCD cleaves opposing strands of DNA by two chemically distinct nuclease reactions. Nucleic Acids Res. 46, 11303–11314. 10.1093/nar/gky878 [PubMed: 30277537]

Schoepfer J, Jahnke W, Berellini G, Buonamici S, Cotesta S, Cowan-Jacob SW, Dodd S, Drueckes P, Fabbro D, Gabriel T, Groell JM, Grotzfeld RM, Hassan AQ, Henry C, Iyer V, Jones D, Lombardo F, Loo A, Manley PW, Pellé X, Rummel G, Salem B, Warmuth M, Wylie AA, Zoller T, Marzinzik AL, Furet P, 2018. Discovery of Asciminib (ABL001), an Allosteric Inhibitor of the Tyrosine Kinase Activity of BCR-ABL1. J. Med. Chem 61, 8120–8135. 10.1021/acs.jmedchem.8b01040 [PubMed: 30137981]

Seifert FU, Lammens K, Stoehr G, Kessler B, Hopfner K-P, 2016. Structural mechanism of ATP-dependent DNA binding and DNA end bridging by eukaryotic Rad50. EMBO J. 35, 759–72. 10.15252/embj.201592934 [PubMed: 26896444]

Sekhar A, Kay LE, 2019. An NMR View of Protein Dynamics in Health and Disease. Annu. Rev. Biophys 48, 297–319. 10.1146/annurev-biophys-052118 [PubMed: 30901260]

Selvaratnam R, Chowdhury S, Vanschouwen B, Melacini G, 2011. Mapping allostery through the covariance analysis of NMR chemical shifts. Proc. Natl. Acad. Sci. U. S. A 108, 6133–8. 10.1073/pnas.1017311108 [PubMed: 21444788]

Selvin PR, 2002. Principles and Biophysical Applications of Lanthanide-Based Probes. Annu. Rev. Biophys. Biomol. Struct 31, 275–302. 10.1146/annurev.biophys.31.101101.140927 [PubMed: 11988471]

Shibata A, Moiani D, Arvai AS, Perry J, Harding SM, Genois M-MM, Maity R, van Rossum-Fikkert S, Kertokalio A, Romoli F, Ismail A, Ismalaj E, Petricci E, Neale MJ, Bristow RG, Masson JY, Wyman C, Jeggo PA, Tainer JA, 2014. DNA Double-Strand Break Repair Pathway Choice Is Directed by Distinct MRE11 Nuclease Activities. Mol. Cell 53, 7–18. 10.1016/j.molcel.2013.11.003 [PubMed: 24316220]

Sprangers R, Kay LE, 2007. Quantitative dynamics and binding studies of the 20S proteasome by NMR. Nature 445, 618–622. 10.1038/nature05512 [PubMed: 17237764]

Stone MJ, 2001. NMR Relaxation Studies of the Role of Conformational Entropy in Protein Stability and Ligand Binding. Acc. Chem. Res 34, 379–388. 10.1021/ar000079c [PubMed: 11352716]

Sun H, Kay LE, Tugarinov V, 2011. An Optimized Relaxation-Based Coherence Transfer NMR Experiment for the Measurement of Side-Chain Order in Methyl-Protonated, Highly Deuterated Proteins. J. Phys. Chem. B 115, 14878–14884. 10.1021/jp209049k [PubMed: 22040035]

Sung S, Li F, Park YB, Kim JS, Kim A, Song O-K, Kim J, Che J, Lee SE, Cho Y, 2014. DNA end recognition by the Mre11 nuclease dimer: insights into resection and repair of damaged DNA. EMBO J. 33, 1–14. 10.15252/embj.201488299 [PubMed: 24399672]

Syed A, Tainer JA, 2018. The MRE11-RAD50-NBS1 Complex Conducts the Orchestration of Damage Signaling and Outcomes to Stress in DNA Replication and Repair. Annu. Rev. Biochem 87, 263–294. 10.1146/annurev-biochem-062917-012415 [PubMed: 29709199]

Tatebe H, Lim CT, Konno H, Shiozaki K, Shinohara A, Uchihashi T, Furukohri A, 2020. Rad50 zinc hook functions as a constitutive dimerization module interchangeable with SMC hinge. Nat. Commun 11, 1–11. 10.1038/s41467-019-14025-0 [PubMed: 31911652]

Tugarinov V, Hwang PM, Ollerenshaw JE, Kay LE, 2003. Cross-Correlated Relaxation Enhanced 1 H − 13 C NMR Spectroscopy of Methyl Groups in Very High Molecular Weight Proteins and Protein Complexes. J. Am. Chem. Soc 125, 10420–10428. 10.1021/ja030153x [PubMed: 12926967]

Tugarinov V, Kay LE, 2004. An Isotope Labeling Strategy for Methyl TROSY Spectroscopy. J. Biomol. NMR 28, 165–172. 10.1023/B:JNMR.0000013824.93994.1f [PubMed: 14755160]

van Noort J, van Der Heijden T, de Jager M, Wyman C, Kanaar R, Dekker C, 2003. The coiled-coil of the human Rad50 DNA repair protein contains specific segments of increased flexibility. Proc. Natl. Acad. Sci. U. S. A 100, 7581–7586. 10.1073/pnas.1330706100 [PubMed: 12805565]

Williams GJ, Williams RS, Williams JS, Moncalian G, Arvai AS, Limbo O, Guenther G, SilDas S, Hammel M, Russell P, Tainer JA, 2011. ABC ATPase signature helices in Rad50 link nucleotide

state to Mre11 interface for DNA repair. Nat. Struct. Mol. Biol 18, 423–431. 10.1038/nsmb.2038 [PubMed: 21441914]

Williams RS, Dodson GE, Limbo O, Yamada Y, Williams JS, Guenther G, Classen S, Glover JNM, Iwasaki H, Russell P, Tainer JA, 2009. Nbs1 flexibly tethers Ctp1 and Mre11-Rad50 to coordinate DNA double-strand break processing and repair. Cell 139, 87–99. 10.1016/j.cell.2009.07.033 [PubMed: 19804755]

Williams RS, Moncalian G, Williams JS, Yamada Y, Limbo O, Shin DS, Groocock LM, Cahill D, Hitomi C, Guenther G, Moiani D, Carney JP, Russell P, Tainer JA, 2008. Mre11 dimers coordinate DNA end bridging and nuclease processing in double-strand-break repair. Cell 135, 97–109. 10.1016/j.cell.2008.08.017 [PubMed: 18854158]

Zabolotnaya E, Mela I, Williamson MJ, Bray SM, Yau SK, Papatziamou D, Edwardson JM, Robinson NP, Henderson RM, 2020. Modes of action of the archaeal Mre11/Rad50 DNA-repair complex revealed by fast-scan atomic force microscopy, Proceedings of the National Academy of Sciences of the United States of America. 10.1073/pnas.1915598117

Zoghbi ME, Altenberg GA, 2018. Luminescence resonance energy transfer spectroscopy of ATP-binding cassette proteins. Biochim. Biophys. Acta - Biomembr 1860, 854–867. 10.1016/j.bbamem.2017.08.005

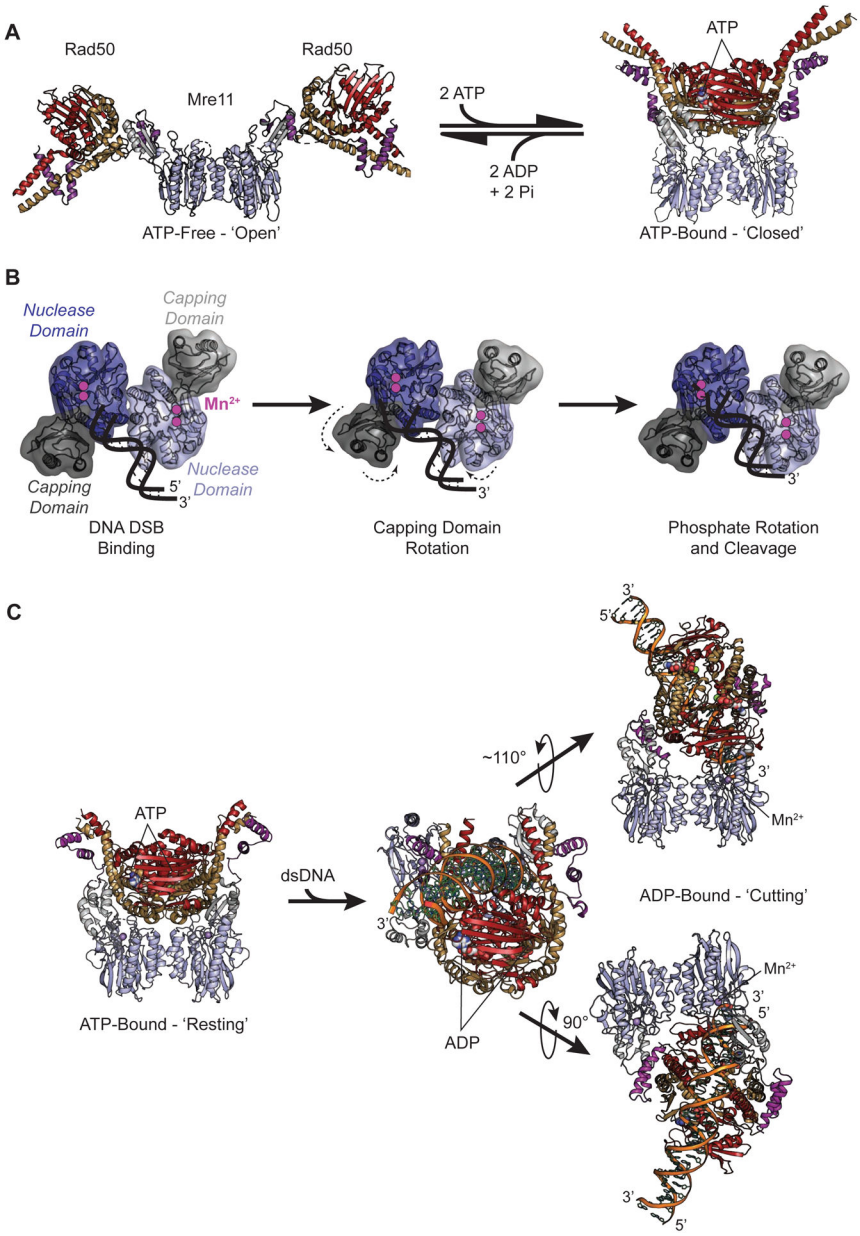

Fig. 1.

Domain motions that are critical for Mre11-Rad50 function. **A)** X-ray crystal structures of *T. maritima* MR complex in the ATP-free 'open' (left; PDB entry 3QG5) and ATP-bound 'closed' (right; PDB entry 3THO) conformations (Lammens et al., 2011; Möckel et al., 2012). For each structure, Mre11 nuclease, capping, and helix-loop-helix domains are colored light blue, grey, and purple, respectively, while Rad50 NBD N- and C-terminal sub-domains are colored red and gold. **B)** X-ray crystal structures of *P. furiosus* Mre11 capping and nuclease domain (PDB entries 3DSC and 3DSD) with nuclease and capping domains colored in blue and grey shades, respectively (Williams et al., 2008). Catalytic Mn^{2+} ions are denoted by magenta circles. The effect of asymmetric domain motions is shown on the cartoon DNA. **C)** Cryo-EM structures of *E. coli* MR (SbcCD) complex in the ATP-bound

‘resting’ state (left; PDB entry 6S6V) and ADP- and dsDNA-bound ‘cutting’ state (right; PDB entry 6S85). Structures are colored as in **A**. Three views of the ‘cutting’ state are presented where the structure has been rotated by the indicated angle.

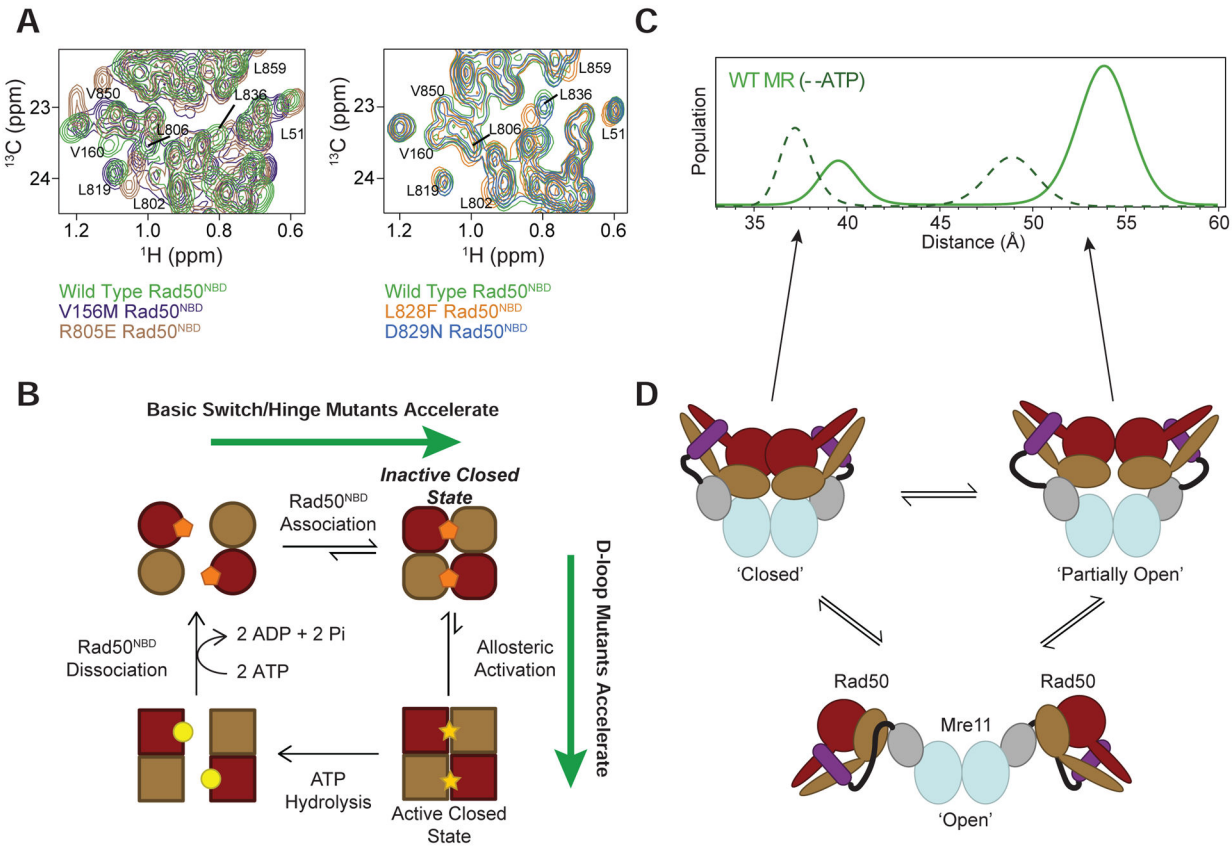

Fig. 2.

Small- and large-scale conformational motions within Rad50 NBDs. **A)** A region of the methyl-TROSY spectra for wild type and basic switch/hinge (left) and D-loop (right) mutants highlighting changes in structure that occur upon perturbation. **B)** Schematic of the structural changes occurring in the Rad50 NBDs during ATP-induced association, hydrolysis, and dissociation. Red and gold shapes symbolize the N- and C-terminal sub-domains of the NBDs, respectively, and the changes in the shapes signify the different states the NBDs must populate to associate, hydrolyze ATP, and dissociate. The pentagons and stars represent ATP, whereas the circles represent ADP. Basic switch and hinge region mutants accelerate the Rad50^{NBD} association step, whereas D-loop mutants accelerate cooperative/allosteric transitions leading to faster ATP hydrolysis. **C)** An example of LRET-derived distance distribution demonstrating a 'partially open' state. ATP binding shifts the equilibrium to favor the 'closed' state and leads to slightly shorter distance between the two probes for both states (dashed line). **D)** Cartoon representation of the new 'partially open' state of the MR complex observed in LRET experiments. Domains of the MR complex are colored according to Figure 1A. Figure adapted from Refs. (Boswell et al., 2020, 2018).

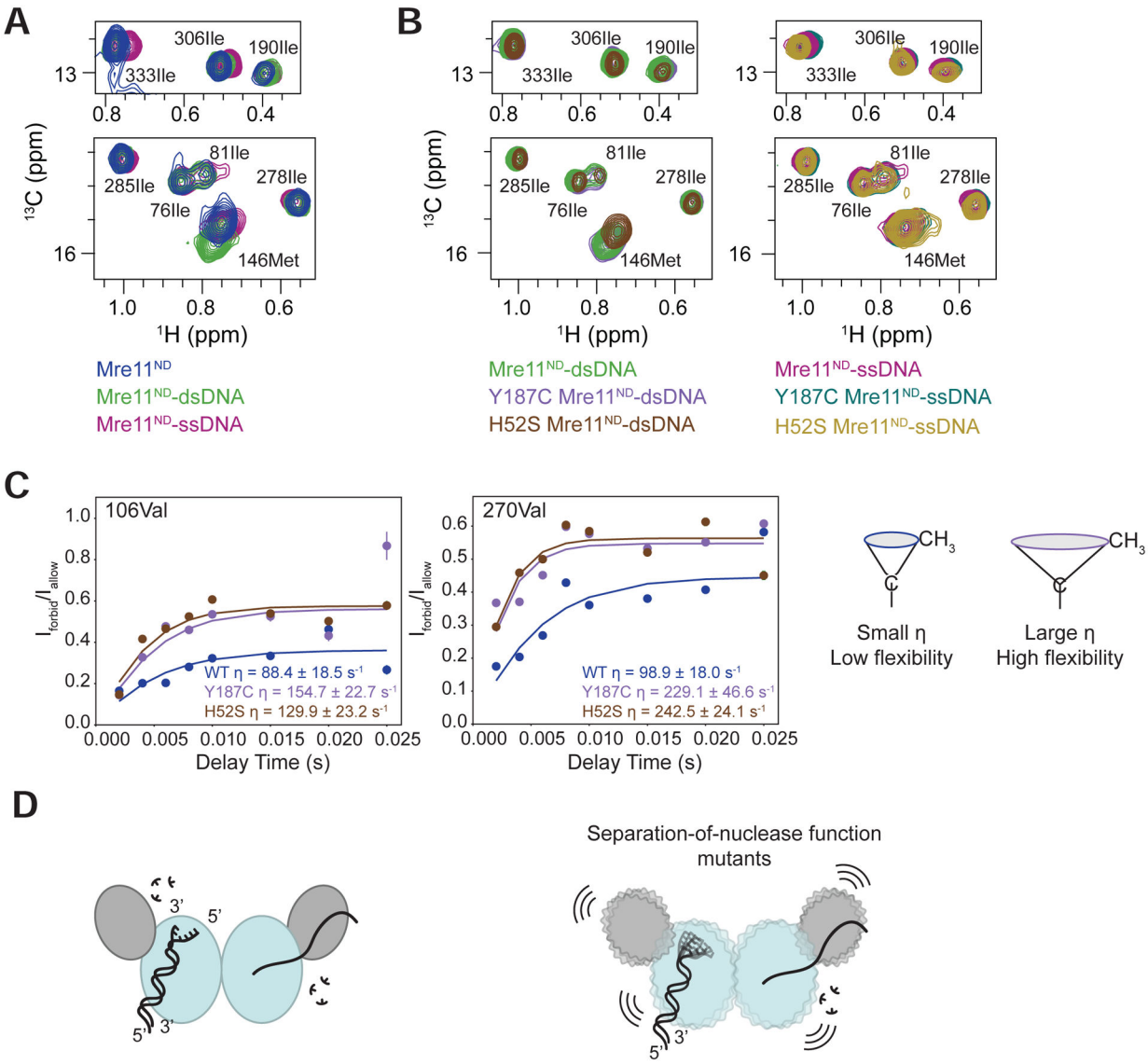

Fig. 3.

Rigid Mre11 recognizes dsDNA substrates for exonuclease activity. **A)** Overlay of the methyl-TROSY spectra indicating that dsDNA and ssDNA substrates cause a single and unique perturbation. **B)** Overlay of the methyl-TROSY spectra showing that the separation-of-nuclease function mutants (*Pf* Mre11ND Y187C and H52S) bind dsDNA (left) differently compared to wild type but ssDNA (right) the same. **C)** Example methyl ^{1}H-^{1}H dipolar cross-correlated triple quantum relaxation data (Sun et al., 2011) for wild type, Y187C, and H52S *Pf* Mre11ND. The extracted relaxation rate (η) reports on the amplitude of side-chain methyl group dynamics as schematically shown to the right. **D)** A cartoon representation of a less flexible Mre11ND that can stably bind and recognize dsDNA and ssDNA substrates for nuclease reactions. Separation-of-nuclease function mutants alter the structure and dynamics of the protein leading to the inability to properly recognize dsDNA substrates. Figure adapted from Ref. (Rahman et al., 2020a).